CONF-890708--5

CONF-890708--5

DE89 015365

ELECTRON CAPTURE AND ENERGY-GAIN SPECTROSCOPY

Knud Taulbjerg

Oak Ridge National Laboratory*
Oak Ridge, Tennessee 37831-6373
and
University of Tennessee
Knoxville, Tennessee 37996-1200

Invited paper to be presented at
XVI International Conference on the Physics of Electronic and Atomic Collisions
New York, New York
July 26 - August 1, 1989

*Research sponsored by the Division of Chemical Sciences, Office of Basic Energy Sciences, U.S. Department of Energy under Contract No. DE-AC05-84OR21400 with Martin Marietta Energy Systems, Inc.

ELECTRON CAPTURE AND ENERGY-GAIN SPECTROSCOPY

Knud Taulbjerg*

Oak Ridge National Laboratory
Oak Ridge, Tennessee 37831-6373
and
University of Tennessee
Knoxville, Tennessee 37996-1200

The applicability of translation energy spectroscopy as a tool to determine individual reaction cross sections in atomic collisions is analyzed with special emphasis on the electron capture process in highly charged ion collisions. A condition is derived to separate between higher collision energies where translation energy spectroscopy is problem free and lower energies where strong overlap of individual spectra features prohibits an analysis of the total translation energy spectrum by means of a simple deconvolution procedure.

I. INTRODUCTION

It is a well-known experimental technique to employ an energy analysis of scattered projectiles or recoiling target atoms to determine differential cross sections for inelastic processes in ion-atom collisions. As a matter of fact, the fundamental studies of inner shell processes in the sixties[1] that stimulated the development of the Fano-Lichten model for ion-atom collisions were performed using this technique. The method is based on the fact that various inelastic channels at fixed scattering angle are separated in the residual energy of the scattered projectile or in the energy of the recoiling target atom by characteristic amounts uniquely related to the corresponding Q-values.

Modern applications exploit that the resolution power of the technique is strongly increased at forward angles to allow a separation of channels that differ by as little as an electron volt in inelasticity. For processes that are dominated by sufficiently small scattering angles, it is possible to record complete differential cross sections for individual inelastic processes as separated features in the spectrum of residual projectile energy without discrimination against scattering angles. The technique is then commonly referred to as translation energy spectroscopy.

It is the purpose of this paper to discuss the applicability as well as the limitations of translation energy spectroscopy with special emphasis on the electron capture process in highly charged ion collisions, in which case the technique is often referred to as energy-gain spectroscopy. First, we briefly review the basic kinematics needed to provide a unique correspondence between differential cross sections and translation energy spectra in collisions of known inelasticity. Next, a qualitative example is considered to illustrate the conditions under which total translation energy spectra can be resolved into individual components corresponding to different intrinsic states. Quantitative applications are discussed at the end.

II. KINEMATICS

The kinematical relations that are needed to determine the energy of a projectile after a collision of given inelasticity, Q_n, are trivial to express in the center-of-mass frame of the two-body collision system. The transformation to the laboratory frame is more complicated but may be completed in closed form (see, for example, Ref. 2). In this work, we shall only be concerned with small laboratory scattering angles, θ, in which case we find to first order in $\sin^2\theta$,

$$\Delta E_n = E_f - E_i = Q_n - \alpha E_i \sin^2\theta, \qquad (1)$$

where E_i and E_f are projectile energies before and after the collision, and Q_n is the amount of inelasticity in the considered reaction channel n, positive for exothermic and negative for endothermic processes. The parameter α is given by

$$\alpha = M_p/M_T + (Q_n/E_i), \qquad (2)$$

*Permanent address: Institute of Physics, Aarhus University, DK-8000 Aarhus, Denmark.

where M_p and M_T are the mass of the projectile and the target, and where the last term can be ignored for all practical purposes in this work. The parameter α is accordingly unity for symmetric systems but becomes much larger than unity in the important case of collisions of highly charged ions with light target atoms or molecules.

The relation given by Eq. (1) may be used to express the translation energy spectrum pertaining to a specific inelastic process, n, in terms of the corresponding differential scattering cross section. By definition, we write

$$\frac{d\sigma_n}{d\Delta E} = \frac{d\sigma_n}{d\theta} \Big/ \frac{d\Delta E}{d\theta}\Bigg|_{\theta = \theta_n(\Delta E)'} \tag{3}$$

Using Eq. (1), we obtain

$$\frac{d\sigma_n}{d\Delta E} = \frac{1}{\alpha E_i \sin 2\theta} \frac{d\sigma_n}{d\theta}\Bigg|_{\theta = \theta_n(\Delta E)'} \tag{4}$$

which is valid at small scattering angles, or, introducing the solid angle $d\Omega = 2\pi \sin\theta d\theta$,

$$\frac{d\sigma_n}{d\Delta E} = \frac{\pi}{\alpha E_i} \frac{d\sigma_n}{d\Omega}\Bigg|_{\theta = \theta_n(\Delta E)} \tag{5}$$

still only valid at small scattering angles. It is seen that the translation energy spectrum at forward angles terminates at $E_f = E_i - Q_n$ for the n^{th} reaction channel and extends towards lower energies with a profile that uniquely represents the corresponding differential scattering cross section $d\sigma_n/d\Omega$. The width of the profile is, according to Eq. (1), proportional to the parameter α. To estimate how the width varies with projectile energy, it is appropriate to consider the reduced scattering angle

$$\rho = E_i \sin\theta, \tag{6}$$

which covers a range which is expected to be insensitive to energy variations since ρ^{-1} is an approximate measure of impact parameters in the type of collisions considered here. Combining Eqs. (4) and (6), we find

$$\frac{d\sigma_n}{d\Delta E} = \frac{E_i}{\alpha} \frac{d\sigma_n}{d\rho^2}\Bigg|_{\rho^2 = (Q_n - \Delta E)E_i/\alpha'} \tag{7}$$

To the extent that the width of $d\sigma_n/d\rho^2$ is independent of energy, it appears that the width, W, of the corresponding structure in the translation energy spectrum is proportional to the parameter α/E_i

$$W \propto \alpha/E_i. \tag{8}$$

Note that α may be varied independently of other relevant parameters by considering different target isotopes.

III. QUALITATIVE EXAMPLE

To illustrate the kinematic transformations discussed in the previous section, we consider a qualitative example where two inelastic channels may be populated. The differential cross

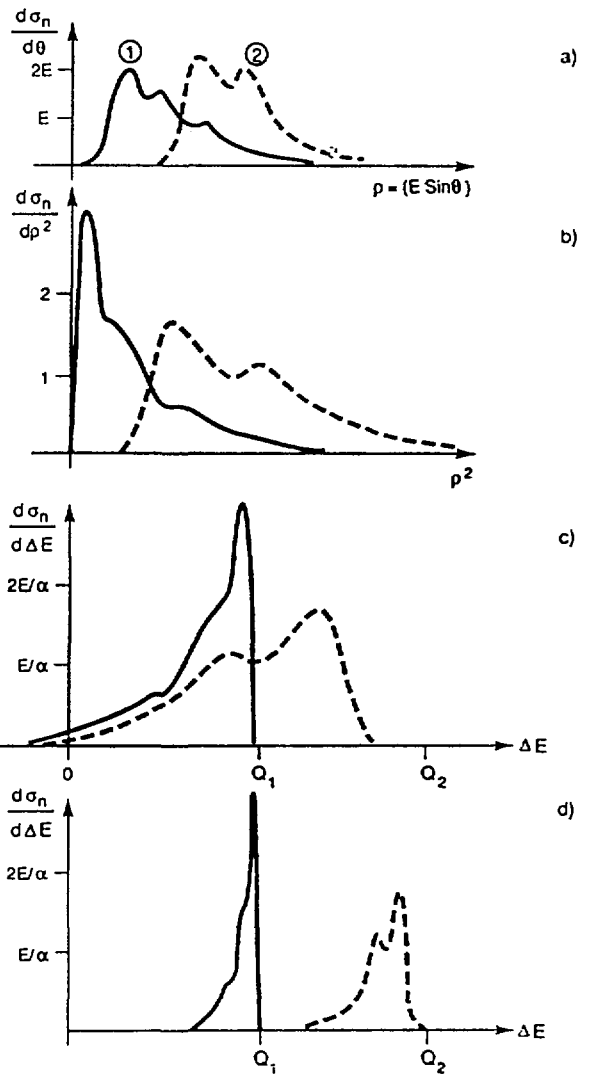

Figure 1. Schematic representation in arbitrary units of differential reaction cross sections and corresponding translation-energy spectra. The mass parameter $\alpha = M_p/M_T$ is a factor of four larger in 1c than in 1d.

sections, $d\sigma_n/d\vartheta$ are shown schematically in Fig. 1a as a function of ρ. The detailed shape of these curves will, of course, vary with energy, but the range of ρ-values which is covered is expected to be characteristic of the impact parameter range, where the two channels are populated and accordingly to be rather insensitive to energy variations. The cross sections given in Fig. 1a are shown again in Fig. 1b as $d\sigma_n/d\rho^2$ versus ρ^2. Notice how reaction 1 appears with a rather sharp feature at small values of ρ^2, while process 2 gives rise to a broader structure. The compression effect at small scattering angles is essential for the resolution power in translation energy spectroscopy.

According to Eq. (7), we may obtain the translation energy spectra by a reflection of the curves in Fig. 1b combined with a suitable scaling of axes and a shift along the energy axis by an amount which equals the Q-value for the considered reaction channel. This is illustrated in Figs. 1c and 1d for two representative values of the α-parameter which, according to Eq. (7) determines the scale parameters for constant energy. The α-parameter in 1c is four times larger than in 1d. The complete scale parameter is, however, given by (α/E_i), and since the range of ρ-values is expected to be insensitive to energy variations, Fig. 1c and 1d also provide a qualitative picture of typical translation energy spectra for a given system (fixed α) at different energies (up by a factor of four in 1d compared with 1c). The resolution may accordingly be increased by using either a heavier target atom or more energetic projectiles.

In practical experiments it is the total translation energy spectrum; i.e., the sum of individual components that is measured. It is therefore essential for a simple analysis of experimental data that individual components are well separated as in Fig. 1d, in which case Eq. (5) can be used directly to extract differential cross sections for the various reaction channels. Similarly, integrated reaction cross sections are correctly represented by the area under the individual components in the spectrum. In case (c), on the other hand, it is not possible to resolve a measurement of the total spectrum unambiguously into individual components, and it is realized that simple procedures to determine the relative population of the two channels are bound to fail, typically with the result that the part of the cross section for process 2 that appears at energies below Q_1 is misinterpreted.

To provide a qualitative estimation of the width of individual components in translation energy spectra, we may consider electron capture in highly charged ion collisions as an example. Using the Landau-Zener model, the relevant range of impact parameters for capture to a state with a specific Q-value is $b \lesssim Z_p Z_T/Q$ in atomic units. The corresponding range of scattering angles is given as $\theta \gtrsim Q/E_i$, which implies that the ρ-parameter is limited to a range between Q and, say, 2Q. The width of the corresponding structure in the translation-energy spectrum is accordingly

$$W = 3\frac{\alpha}{E_i} Q^2. \tag{9}$$

Spectral overlap is avoided if

$$W < \Delta Q = Q_n - Q_{n-1}. \tag{10}$$

This implies that the condition

$$E_i > 3\alpha\, Q^2/\Delta Q \tag{11}$$

must be satisfied to ensure a non-overlapping spectrum. In a typical case we may have

$$Q \lesssim 20 \text{ eV} \quad , \quad \Delta Q \gtrsim 3 \text{ eV},$$

which implies that

$$E_i(\text{keV}) \gtrsim \alpha/2$$

to separate the features in the translation energy spectrum. The condition in Eq. (11) is satisfied in most experimental situations for symmetric systems ($\alpha = 1$) but not at lower collision energies in the case of light targets like helium or hydrogen. This conclusion is, of course, somewhat disappointing since studies of highly charged ions in collision with light targets, and especially with atomic hydrogen or its heavier isotopes, are of particular interest. Note, however, that spectral overlap does not mean that translational energy spectroscopy is useless. It only means that some spectral information must be provided to analyze experimental data or that a comparison with theory is to be made directly at spectral levels. A quantitative example is considered in the following section.

IV. QUANTITATIVE RESULTS

The qualitative discussion above will now be substantiated by quantitative results. As an example, we consider experimental translation energy spectra obtained by Giese et al.[3] The data shown in Fig. 2 represent electron capture in collisions of Ar^{+6} with argon and with molecular and atomic deuterium at 3.27 keV. The shape of the experimental spectra is, to a large extent, determined by the experimental resolution which is about ±1 eV, but the effect of the variation of the mass parameter $\alpha = M_p/M_T$ is seen in the data. The width parameter is estimated by Eq. (9) as $W \lesssim \alpha/3$ eV. The individual spectral features are accordingly much narrower

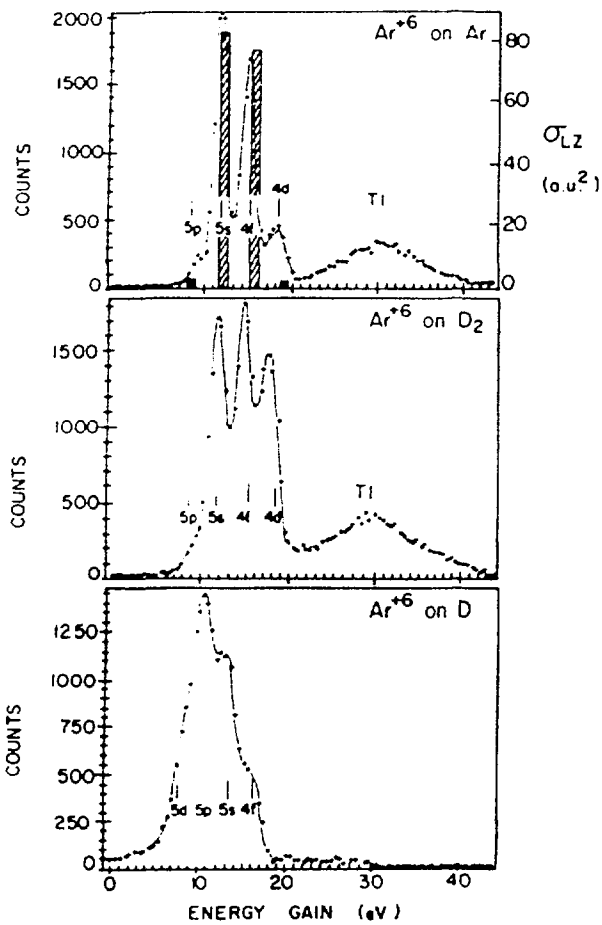

Figure 2. Experimental energy gain spectra in Ar^{+6} electron capture collisions at 3.27 keV impact energy (reproduced from Ref. 2).

than the experimental resolution in case of argon targets. The experimental resolution is, however, fine enough to separate between different Q values. A simple fitting procedure determined by the experimental resolution function is accordingly quite adequate to determine individual reaction cross sections or the relative population over final states of the captured electron. In case of atomic deuterium, on the other hand, the mass parameter α equals 20. This implies that individual contributions are expected to be spread out by up to 7 eV or so. More detailed information about the shape of the spectral contributions is therefore required to analyze the data. This is clearly a task for theory.

To provide the required theoretical information, Hansen and Taulbjerg[4] have used the simple coupled-channel model developed by Larsen and Taulbjerg,[5] combined with an eikonal transformation to determine theoretical energy-gain spectra for Ar^{+6}-D(1s) collisions. Briefly, the model employs an expansion of the time-dependent Schrödinger equations in a basis of projectile and target states and a Galilean-invariant first-order treatment of electron translation factors. Final states on the projectile are modeled by a quantum defect wavefunction of the Bates-Damgaard type. The parameters of the model are accordingly determined only by the binding energies of the various states. These are known experimentally or may be derived by interpolation methods. The first-order treatment of translation factors allows the coupling elements to be pre-evaluated in a suitable mesh of internuclear separations independent of collision velocity and impact parameter. This is essential to reduce the time consumption in large-scale multi-channel calculations. The approximation is sufficiently accurate (see Fig. 2 of Ref. 5) in the velocity range considered in this work. A further, essential reduction in computation time is gained by employing the pre-orthonormalization procedure described in Ref. 6.

Convergence is tested by varying the size of the basis. In our experience, it is generally important to include complete principal shells to allow appropriately for the combined effect of Stark mixing and rotational coupling. In the Ar^{+6}-D(1s) case, this means inclusion of complete n=4 and n=5 principal shells in the ArVI $1s^2 2s^2 2p^6 3s^2 n\ell$ configuration. This corresponds to a total of 26 reflection symmetric states in the basis. Some of these states are not significantly populated after the collision, and it may be expected that the corresponding states could be eliminated if a molecular expansion was used. The larger atomic basis is, however, a low price to pay to avoid the practical problems in connection with the generation of molecular wavefunctions and coupling elements, and, more importantly, the principal problems with the choice of molecular translation factors.

The coupled channel calculations provide electron capture amplitudes $a_f(\underline{b})$ for each of the considered states in a suitable mesh of impact parameters $\underline{b}$. Capture probability functions, defined as sums over magnetic substates,

$$P_f(b) = \sum_{m_f} \left| a_f(\underline{b}) \right|^2$$

and partial cross sections

$$\sigma_f = 2\pi \int_0^\infty b\,db\, P_f(b)$$

are then readily obtained. Capture probability curves for the most important final states are shown in the lefthand panels of Fig. 3. These P(b) curves are characteristic of the primary

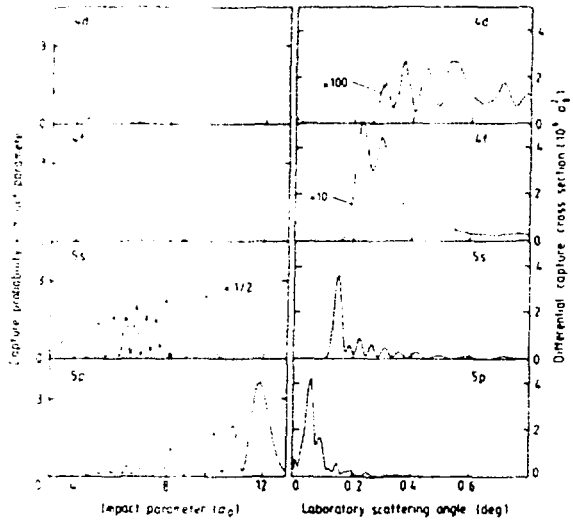

Figure 3. Results from the 26-state calculation of capture in Ar^{6+}-D collisions at 3.27 keV. The lefthand side presents the dependence on impact parameter for the four dominant channels. The righthand side presents the corresponding differential cross sections in the eikonal approximation.

potential curve crossing mechanism for electron capture in highly charged ion collisions. This mechanism controls the regular phase interference oscillations and determines the effective cut-off in the P(b) curves at large impact parameters.

To determine the differential capture cross sections, the capture amplitudes $a_f(\underline{b})$ are amended appropriately by phase factors due to elastic scattering potentials not included in coupled-channel calculations with straight-line trajectories and Bessel transformed to obtain corresponding scattering amplitudes in the eikonal approximation.[7] The resulting differential cross sections are shown in the panels to the right in Fig. 3. Note that the phase interference oscillations also appear in the inelastic scattering cross sections.

Now it is a simple matter to derive theoretical energy gain spectra by aid of the exact relation in Eq. (3). These are shown in Fig. 4. We notice that the dominant lines exhibit a characteristic asymmetric shape with a tail to the low-energy side. The tail is relatively more important in final states with higher Q-values, plainly reflecting that these states are populated in more close encounters. Note, in particular, that the 4d state gives rise to a very broad feature without any reminiscence of a line structure. Generally, we observe that the tails of the spectra extend below the threshold of the adjacent line. The corresponding

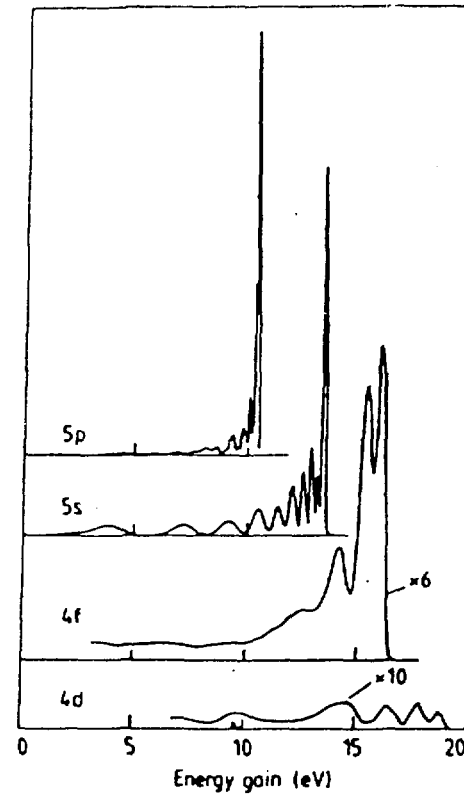

Figure 4. Calculated (26-state) energy-gain spectra for the four dominant capture channels in Ar^{6+}-D collisions at 3.27 keV.

fractions of the reaction cross sections are likely to be misinterpreted in a simple analysis of the summed spectrum. The 4d state, in particular, would be entirely misrepresented since only a small fraction of the 4d cross section appears above the rather sharp threshold for the 4f state in the energy-gain spectrum.

The complete energy-gain spectrum is obtained by summation of the individual components in Fig. 4. To compare with the experimental data, we have modeled the experimental resolution function by a Gaussian with a standard deviation of 1 eV. The theoretical spectrum folded with this resolution function is shown in Fig. 5 in comparison with the experimental data. Apart from the deviation below 5 eV, which originates from the small impact parameter contribution to the 5s channel, the comparison is well within the experimental uncertainties. The theoretical result for the distribution over final states

$$4d:4f:5s:5p = 8:29:44:18 \qquad (12)$$

is accordingly also strongly supported by the

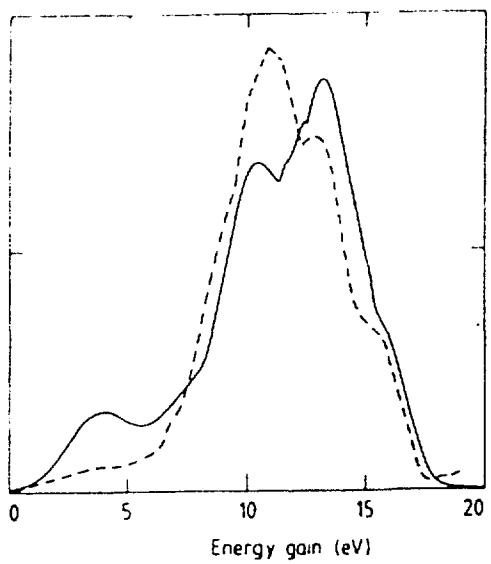

Figure 5. Experimental (broken curve) and theoretical (full curve) energy-gain spectra in Ar^{6+}-D collisions at 3.27 keV. The theoretical spectrum has been folded with a Gaussian resolution function with a standard deviation of 1 eV.

experimental data. This is particularly interesting since a fitting procedure based on Gaussian profiles provides the following distribution: [3]

$$4f:5s:5p:5d = 12:28:41:9. \qquad (13)$$

This distribution is similar to the one in Eq. (12) but it is shifted one unit in the final state assignment. This plainly just reflects the fact that the 4d state is spread out over the whole spectrum and therefore is lost on the high energy side of the structure and that the tails of the strongly populated lines accumulate on the low energy side in the region normally assigned to the 5d level.

We have expanded our calculations to a wider range of Ar^{+6} impact energies in collisions with atomic hydrogen and compared with the experimental data by Afrosimov et al.[8] on the distribution over final states, derived from energy-gain spectra, presumably by a simple deconvolution procedure. There is a consistent departure at lower energies (E < 20 keV) between these distributions and the calculated ones. The trend is similar to the departure described in detail above. At higher energies (E = 20-40 keV) there is good agreement between experiment and theory. This is quite understandable from the spectral shapes in Fig. 4, considering that the width of the individual features is expected to be reduced by a factor of 5 at E ~ 30 keV.

The effect of overlapping features is not peculiar to hydrogen or deuterium targets. This is illustrated in our final example where we consider single electron capture in Ar^{+6}-He collisions. Theoretical energy-gain spectra are shown in Fig. 6 for two impact energies. Our qualitative considerations in Section III are clearly confirmed by the observed energy dependence of the width of the individual spectral features. The overlap between the spectral components is not insignificant in Fig. 6a. As before, this implies that a careful analysis of experimental data is needed to derive the

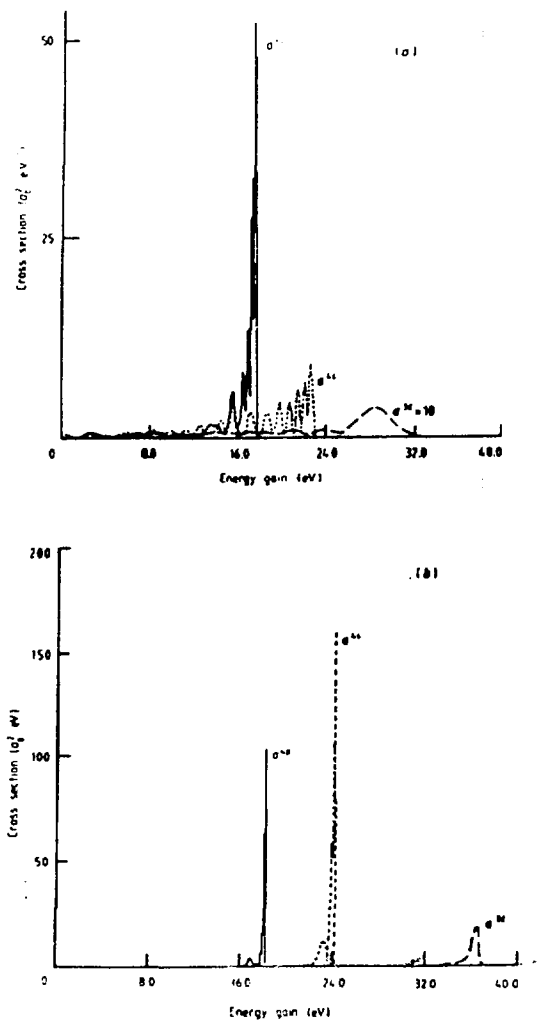

Figure 6. (a) Calculated theoretical energy-gain spectra for the three dominant channels in Ar^{6+}-He collisions at 3.27 keV. (b) Calculated theoretical energy-gain spectra for the three dominant channels in Ar^{6+}-He collisions at 40 keV.

distribution over final states. Generally, cross sections with high Q-values tend to be underestimated in a simple experimental analysis.

The general conclusion of the quantitative computations and of the comparison with available experimental data is in good accord with the qualitative considerations in Section III. In particular, it appears that the condition

$$E \gtrsim 3M_p \, Q^2/M_T \, \Delta Q \qquad (14)$$

has been substantiated to separate between the region at higher impact energies where translation energy spectroscopy is essentially problem free from the region at lower energies where a very careful treatment is needed to provide an unambiguous analysis of experimental spectra.

In the low-energy region it is best to accept theoretical results for the distribution over final states until a sound analysis of experimental data has been performed.

ACKNOWLEDGEMENTS

This research was sponsored by the U.S. Department of Energy, Office of Basic Energy Sciences, Division of Chemical Sciences, under contract No. DE-AC05-84OR21400 with Martin Marietta Energy Systems, Inc.

REFERENCES

1. V. V. Afrosimov, Yu. S. Gordeev, M. N. Panov, and N. V. Fedorenko, Sov. Phys. Tech. Phys. 9, 1248 (1965); Q. C. Kessel and E. Everhart, Phys. Rev. 146, 16 (1966); E. Everhart and Q. C. Kessel, ibid. 146, 27 (1966).
2. E. H. Nielsen et al., J. Phys. B18, 1789 (1985).
3. J. P. Giese et al., Phys. Rev. A34, 3770 (1986).
4. J. P. Hansen and K. Taulbjerg, J. Phys. B21, 2459 (1988).
5. O. G. Larsen and K. Taulbjerg, J. Phys. B17, 4523 (1984).
6. J. P. Hansen and K. Taulbjerg, Comp. Phys. Comm. 51, 317 (1988).
7. R. McCarroll and A. Salin, J. Phys. B1, 163 (1968).
8. V. V. Afrosimov, A. A. Basalaev, K. O. Lozhkin, and M. N. Panov, JETP Lett. 46, 107 (1987).